Ultrafast Electron-Transfer and Solvent Adiabaticity Effects in Viologen Charge-Transfer Complexes

Aravindan Ponnu, Jiha Sung, and Kenneth G. Spears*

Chemistry Department, Northwestern University, Evanston, Illinois 60208-3113

Received: March 20, 2006; In Final Form: July 17, 2006

We report ultrafast electron transfer (ET) in charge-transfer complexes that shows solvent relaxation effects consistent with adiabatic crossover models of nonadiabatic ET. The complexes of either dimethyl viologen (MV) or diheptyl viologen (HV) with 4,4′-biphenol (BP) (MVBP or HVBP complexes) have identical charge-transfer spectra and kinetics in ethylene glycol with ∼900 fs ET decay. We assign this decay time as largely due to adiabatic control of a predicted ∼40 fs nonadiabatic ET. The MVBP decay in methanol of 470 fs is reduced in mixtures having low (2−20%) concentrations of acetonitrile to as short as 330 fs; these effects are associated with faster relaxation time in methanol and its mixtures. In contrast, HVBP has much longer ET decay in methanol (730 fs) and mixture effects that only reduce its decay to 550 fs. We identify the heptyl substituent as creating major perturbations to solvent relaxation times in the methanol solvation shell of HVBP. These charge-transfer systems have reasonably well-defined geometry with weak electronic coupling where the electronic transitions are not dependent on intramolecular motions. We used a nonadiabatic ET model with several models for adiabatic crossover predictions to discuss the small variation of energy gap with solvent and the ET rates derived from adiabatic solvent control. A time correlation model of solvent relaxation was used to define the solvent relaxation times for this case of approximately zero-barrier ET.

I. Introduction

A. Overview. In general, the role of solvent relaxation times on electron-transfer (ET) kinetics is expected to be large for adiabatic ET and less important for nonadiabatic ET, and this has been discussed in recent reviews.[1−3] A number of models have been developed to add solvent relaxation contributions to a nonadiabatic ET rate, and these rate expressions also use solvent relaxation parameters to crossover into a full adiabatic description in slow relaxing solvents.[4−9] Experiments that identify solvent dynamic control of ET are in the literature,[10−15] and most of these studies have identified molecules where the solvent relaxation is controlling charge reorganization kinetics on relatively slow time scales. These ET systems often are intramolecular charge rearrangements, sometimes coupled to intramolecular motions, and usually with strong electronic coupling. Ultrafast, nonadiabatic ET often shows negligible solvent control due to the role of vibrational reorganization energy and its nonclassical effects on rate.[1,2,16−20] Examples of ultrafast, nonadiabatic ET that also demonstrate solvent relaxation effects are desirable to study for testing theoretical models. The best ET system to study adiabatic solvent effects would have well-defined geometry with weak electronic coupling, electronic transitions not dependent on intramolecular motions, and electronic states weakly coupled to the solvent. For this case standard nonadiabatic rate constant models can be used to model ultrafast ET rates in the zero-barrier or slightly inverted region of ET, and according to current models we expect to observe crossover to adiabatic solvent relaxation control. In this work we show that this regime of ET can reveal many details of solvent control of ET.

This work is a continuation of prior work from this laboratory that investigated electron transfer in the same viologen charge-transfer complexes but only in methanol solution.[21] That work and the current work use optical excitation of a charge-transfer (CT) absorption band with femtosecond pulses and then monitors transient absorption spectra of the viologen radical cation to observe the return electron-transfer rates. The optical excitation converts the viologen doubly charged cation into a delocalized singly charged cation and a new biphenol cation to form a new complex with two charges that are more delocalized than the initial complex. The goal of the prior study was to compare two similar molecules whose return electron-transfer rates should have been identical if energetic parameters, inferred from a variety of spectroscopic methods, were controlling the rates. We studied charge-transfer complexes of dimethyl viologen (MV) and diheptyl viologen (HV) with 4,4′-biphenol (BP) (complexes are labeled MVBP and HVBP) in methanol; structures of the viologen framework and biphenol are shown in Figure 1, where R is methyl for MV and heptyl for HV. In our prior work we found a 65% larger ET rate for the MVBP complex, and this result was interpreted as due to adiabatic effects, since solvent relaxation times are on the same time scale as the 480 and 790 fs decay times of MVBP and HVBP, respectively. The model used a full solvent correlation function to compute the type of adiabatic contributions that might be present in HVBP. We conjectured that local solvent order involving the heptyl group was the main effect on the methanol solvent reorganization time.

In this work we sought other solvents for the same complexes that could reveal both solvent reorganization and energetic influences on ET rates. For experimental studies of charge-transfer complexes, one seeks concentrations where the sample is dominated by ion pairs at high concentrations of 0.1−0.2 M. We recently found that ethylene glycol and dilute solvent mixtures in methanol could provide new insight into the ET kinetics. One goal was to find a solvent where we observe the

* Corresponding author. E-mail: k-spears@northwestern.edu.

10.1021/jp0617322 CCC: $33.50
Published on Web 10/17/2006

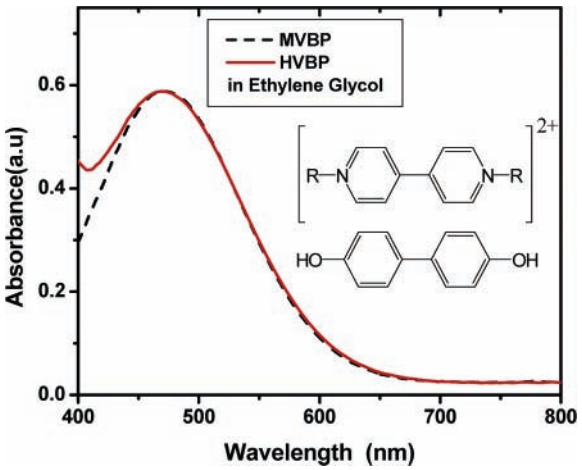

Figure 1. Absorption spectra of MVBP and HVBP complexes in ethylene glycol. The R group defines the viologen (R is $-CH_3$ for MV and $-(CH_2)_6CH_3$ for HV).

predicted identity of ET rates, which unequivocally would establish the premise of similar ET energetics and similar ET rates for the two viologen complexes. A second goal was to measure ET rates in solvent mixtures that have small perturbations of methanol solvent structure. A third goal was to compare different theoretical models for the crossover between nonadiabatic and adiabatic ET with our data. We will show in the following sections that these complexes clearly show solvent reorganization control of ET on an ultrafast time scale and that current models can approximately explain the observed data. Additional theoretical and experimental work is desired for understanding the crossover to ultrafast adiabatic ET.

B. Solvent Effects in Electron Transfer. The history of solvent relaxation in ET is too large to be reviewed here completely. A recent two-volume set of reviews[1−3] on many aspects of ET is quite useful; in this work Bixon and Jortner[1] discuss solvent relaxation effects with emphasis on those ultrafast ET cases which do not manifest solvent control.

In general, solvent control appears to be most important for ET where small to normal activation energy is required and vibrational reorganization is not dominating the rates (low exothermicity usually implies less importance for this factor). This type of ET is often intramolecular and involves electronic states having different charge distributions within a molecular framework. Often there is strong coupling between these states, and intramolecular motion may be coupled to the ET coordinate so that the coupling and energy positions can be a function of the ET coordinate. A two-state adiabatic model is often a severe approximation for such systems, but the adiabatic character of the experimental behavior (not necessarily a simple ET coordinate) is clearly related to solvent relaxation by studies in solvents having a wide range of solvent polarity and solvent hydrogen bonding. The case of bianthryl[12,22,23] was modeled with a generalized Langevin diffusion model for adiabatic potentials consistent with spectra and solvent friction consistent with solvent effects on spectral relaxation. However, recent work[24] has suggested the mechanism in bianthryl is more complex; they propose an intrinsic ET on the 1−10 fs time scale (consistent with direct excitation), which then has a solvent relaxation that is associated with the energy gap between the two states rather than a mixed ET and solvent coordinate. Recent work on a similar type of ET involving a local state to charge-transfer state[13] has shown solvent control related to relaxation times of the solvation probe Coumarin 153 via a power law. As these examples show, understanding the details of solvent control of ET has some experimental complexities since the coordinate for ET may depend on molecular motions and solvent motions and might have a large coupling matrix element that also could be a function of this complex coordinate.

If we consider the case of ultrafast ET, one finds a number of cases where the rate is much faster than the solvent relaxation time.[1,2,16−20] These cases often are highly exothermic and can have significant vibrational reorganization energy so that the ET rate is better described with a quantum model having energy-accepting vibrational modes; this model allows a much faster rate than predicted from classical solvent reorganization. For betaines[25,26] the ET is an intramolecular charge reorganization with a charge-transfer band that indicated a fairly strong coupling matrix element of $\sim$1400−2800 cm^{-1}. The small solvent dependence seen in the initial studies is characteristic of the quantum model of ET, and a nonadiabatic model could approximately explain the magnitude of the rates. However, the large coupling is outside the expected validity range for a nonadiabatic ET model. A recent study[27] has identified the ET as having an initial ultrafast step with two components whose times approximately correlate with solvent relaxation models for acetonitrile and methanol. For example, the times in picoseconds with amplitudes in parentheses are 0.07 (0.70) and 0.33 (0.30) in AN and 0.048 (0.48) and 0.38 (0.52) in MeOH. These values give an "average" ET time (by weighting the rates) as 0.092 and 0.09 ps, respectively. The EG solvent gives a time of 2.3 ps, and EtOH has an average value of 0.48 ps. In this case it appears that solvent control might be operating for some solvents, but EtOH and EG are less closely associated with solvent reorganization. These recent results suggest a new mechanism of ultrafast ET in betaine that does have a solvent reorganization component on the ultrafast time scale. While more work needs to be done in understanding this molecule, it is a strongly coupled system with reasonably large exothermicity in the inverted ET regime whose ultrafast character does not fall into a simple model of ET. However, the fast ET in other very slow relaxing solvents[25,26] suggests that vibrational modes and a quantum model[28] are important components of the mechanism.

Solvent control of ET in another ultrafast ET system was demonstrated for quenching studies of the rhodamine 800 excited state, where the quenching is by ET to one component of a solvent mixture. While this system does not have a well-defined initial geometry of the two components, the solvent mixtures of acetonitrile and dimethylaniline did allow tuning of the ET quenching time in the 1−5 ps time scale, and this range of times was correlated with τ_L for the solvent mixtures.[29] In contrast to this case, similar quenching studies in other molecules show ultrafast ET with little evidence for solvent relaxation effects.[2]

Some of the best systems for study of ultrafast ET, where solvent control appears to not be present, are metal−metal charge-transfer complexes. One intramolecular case, with very strong coupling, only shows small solvent effects; for example, water and ethylene glycol have multicomponent ET times of $\sim$100 and $\sim$220 fs, respectively.[10,30] The case of strong coupling is more difficult to model, but this case seems to support the absence of large solvent relaxation effects that can correlate with solvent relaxation.

As indicated in the discussion of the betaine experiments, ultrafast ET rates need to be examined carefully since adiabatic behavior might occur even with very fast ET. Our earlier report on these viologen CT complexes[21] identified solvent control of

ET for subpicosecond times. We will discuss this system in more detail below.

II. Experimental Methods

The methods were very similar to our prior work.[21] Kinetic measurements were made by optically pumping the charge-transfer absorption near 490 nm and then monitoring the decay of the viologen radical cation near its peak absorbance of 615 nm.[31] Experiments were carried out using an amplified Ti: sapphire laser system described in a prior publication.[32] The 60−90 fs output of the compressor is centered at 805 nm with a spectral bandwidth of ∼22 nm. A laboratory-built near-IR optical parametric amplifier (OPA) is summed with 805 nm to generate an ∼500 nm pump beam (2 μJ/pulse) with a spectral bandwidth of ∼15 nm. Continuum probe pulses were generated by focusing the compressed 800 nm beam into a 3 mm thick piece of optical-grade sapphire with a 15 cm focal length lens. Both 2 and 5 mm cell paths were used for the transient absorption; the concentration of the sample was maintained at 0.20 and 0.15 M, respectively. The sample was not flowed, and signals were stable over a wide range of time. Pump and probe beams crossed at an angle of 5° and were focused to spot sizes of 600 and 300 μm, respectively. After the sample the probe beam was filtered by a short-pass interference filter (<750 nm) and coupled into an Ocean Optics spectrograph using an optical fiber. The scattered pump beam was blocked by an Ocean Optics LP495 tunable interference filter. The filter was placed before the optical fiber. Transient absorption from 400 to 750 nm over a time range from 0 to ∼4 ps was done using alternating pump on/off pulses with electronics and software by Ultrafast Systems Inc. The system rise time was determined for each sample by fitting rhodamine 6G transient kinetics, and the resultant effective pulse width was used in fitting the ET kinetics.

The chemicals 1,1′-dimethyl-4,4′-bipyridinium dichloride hydrate, 1,1′-diheptyl-4,4′-bipyridinium dibromide, and 4,4′-biphenol were purchased from Aldrich and used as received. Methanol (MeOH), ethylene glycol (EG), acetonitrile (AN), and ethanol (EtOH) were purchased from Fisher. Solutions of MVBP and HVBP were prepared using 1:1 ratios of the BP and viologen components. All solvents and solvent mixtures were studied as a function of concentration to be sure of solubility and to define a well-behaved extinction coefficient at the maximum concentration of our kinetics experiments.

III. Results

The solutions in EG and dilute mixtures in MeOH were well behaved up to 0.2 M concentration, where our prior study[21] established identical equilibrium constants for MVBP and HVBP. The spectra of these complexes in EG are shown in Figure 1, where similar to MeOH the HVBP shows absorption from a higher energy band on the blue edge of the absorption. Figure 2 gives examples of how solvent polarity changes the CT absorption of MVBP and HVBP for MeOH, EG, and MeOH with 20% acetonitrile (AN) by volume. The wavelength shifts with solvent are small, with EG providing the largest shift relative to MeOH. Tabulating peak shifts is very difficult for such small shifts and wide bands, and small changes in peak shapes reduce the accuracy for mixtures with MeOH. This type of spectral inhomogeneity is very minor, but in order to compare solvent mixtures in MeOH a different method of judging the "peak center" is defined using the midpoint of the peak at a lower optical density of 1.5. For HVBP, only the peak maximum is available for comparison, and we also use the peak maximum for EG in both MVBP and HVBP. For HVBP the shape of the red edge of the spectra is similar for all solvents, which suggests that any changes in the blue edge are not affecting the peak location. These results are tabulated in Table 1, where the main observations are that the HVBP peak is slightly red shifted from MVBP in MeOH and that in EG solvent both MVBP and HVBP have the same peak location. For MVBP the MeOH mixtures with EtOH and AN have much smaller shifts than for EG. For HVBP there is a larger shift in the EtOH mixtures, and all have a negative sign, which is different than the EtOH mixtures for MVBP, which have a small positive sign.

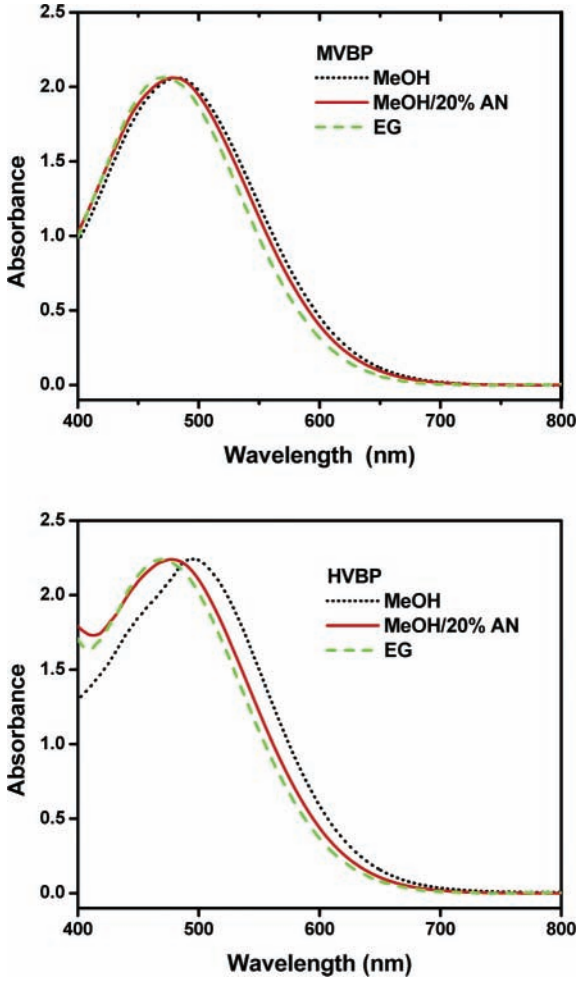

Figure 2. Absorption spectra of MVBP and HVBP in pure and mixed binary solvents at 0.2 M methanol (MeOH), acetonitrile (AN), and ethylene glycol (EG).

The transient absorption kinetics of ET is nominally single exponential in most cases but with small deviations that are insufficiently large to define any other kinetic components with a nonlinear least-squares method. In Figure 3 we show the transient absorption decays of MVBP and HVBP in EG solvent with the model fits for single exponentials. In Figure 4 we show the transient spectra for MVBP and HVBP in EG solvent. The dominant spectral absorption band is for the viologen radical cation; for HVBP and MVBP the radical cation spectra are quite similar, and differences in these spectra are similar to the experimental variations. In Figure 5 we show the MVBP and HVBP transient absorption kinetics in MeOH with 2% AN, which have small but observable changes in decay rate (especially for HVBP) when compared with the expected decay curve for pure MeOH at the same excitation pulse conditions. In Figure 6 we show the transient absorption kinetics of MVBP in MeOH with 5% AN with its exponential fit and an expected decay curve for pure MeOH data. In Figure 7 we show the

TABLE 1: Peak Position of Charge-Transfer Bands and Their Relative Shifts with Solvent

	MVBP[b]	rel MeOH[d]	rel EG[d]	HVBP[c]	rel MeOH	rel EG
solvent[a]	λpeak (nm)	$\Delta\lambda$	$\Delta\lambda$	λpeak (nm)	$\Delta\lambda$	$\Delta\lambda$
MeOH	481.8	0	13.3	494.5	0	25.9
EG	468.5	−13.3	0	468.6	−25.9	0
MeOH/AN(5%)	483	1.2	14.5	485.8	−8.7	17.2
MeOH/AN(10%)	481.2	−0.6	12.7	485.5	−9	16.9
MeOH/AN(20%)	477.9	−3.9	9.4	477.7	−16.8	9.1
MeOH/EtOH(10%)	483.8	2	15.3	491.7	−2.8	23.1
MeOH/EtOH(20%)	484.3	2.5	15.8	490.3	−4.2	21.7

[a] Solvents are as follows: methanol, MeOH; ethylene glycol, EG; acetonitrile, AN; ethanol, EtOH. [b] MVBP peak positions by midpoint of peak at O.D. 1.5; EG uses the peak maximum. Uncertainty in peak location ≈ 0.5 nm. [c] HVBP peak positions by maximum of peak. Uncertainty in peak location ≈ 0.5 nm. [d] rel means relative to (MeOH or EG) peak wavelength.

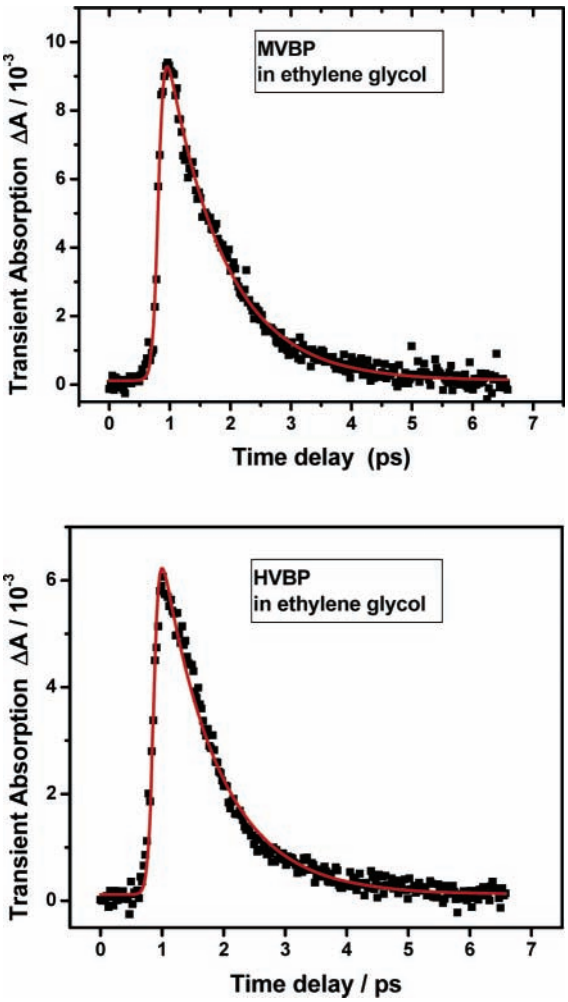

Figure 3. Transient absorption kinetics of MVBP and HVBP in ethylene glycol of the viologen radical cation. The solid curve (red) is a fitted single exponential of 900 (MVBP) and 885 fs (HVBP). The pump and probe wavelengths are 490 and 600 nm, respectively.

transient absorption kinetics for MVBP and HVBP data in MeOH with 20% AN to show how these mixtures fit with one exponential. All of the kinetic fits have small nonexponential behavior, which allows us to tabulate the results as single exponential for simple comparison.

The transient kinetic analysis is in Table 2, with error estimates based on output of the nonlinear least-squares fitting routine (Marquardt algorithm), which are also consistent with averaging over multiple experiments. We note that our earlier report[21] had values in MeOH slightly different from these results but within the error estimates. We tabulate the ratio of decay times and its standard error to show when a change in decay is

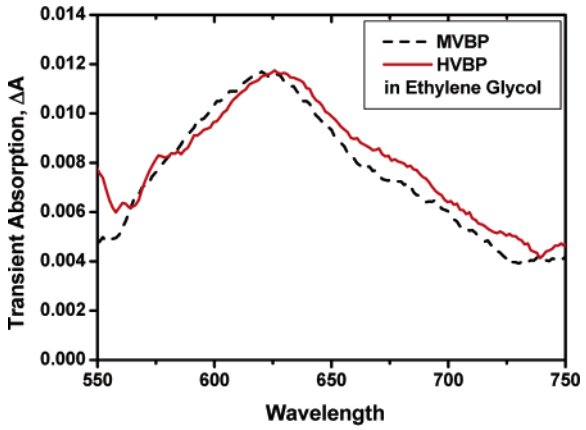

Figure 4. Transient absorption spectra for the MVBP (black) and HVBP (red) radical cations at the time delay for peak absorbance. These spectra are averaged over five time points in a 104 fs interval to reduce noise.

significant. The ET decay times in MeOH with 2% AN show a significant reduction for HVBP and MVBP, but MVBP is only at the one standard deviation level. An additional increase of AN to 5% shows further change in the decay, but little additional change occurs from 5% to 20% AN for MVBP. The EtOH mixtures for HVBP show little significant effect on decay time, while for MVBP the 5% mixture with EtOH shows less change than the 5%AN example.

In Figure 8 we show the transient spectra of MVBP in MeOH for different points in the rise time to the peak. Aside from the earliest time point, there is a broader transient that is progressively narrowing on the blue edge while also shifting and creating a weak feature at 700 nm. The times after the peak are shown in the second part of Figure 8, which show very little shifting and some increase at 700 nm. We have not applied a chirp correction for the typical blue lagging of red probe colors in the white light pulse. In Figure 9 we show the time points before the peak for MVBP in EG, which is similar to MeOH. The EG solvent data shows less spectral shifting over the 100 fs rise time than the MeOH solvent data but similar narrowing.

IV. Discussion of Data

A. Overview. Our prior work established the basic parameters of an ET model for these systems and the constancy of the coupling matrix element. The two complexes have identical extinction coefficients in MeOH and other solvents, which implies that the small solvent energy level shifts are not simultaneously making large changes in the geometry of the complex and the coupling matrix element. In the following discussion we will show that expected ET rates in a pure nonadiabatic model and the computed solvent relaxation times

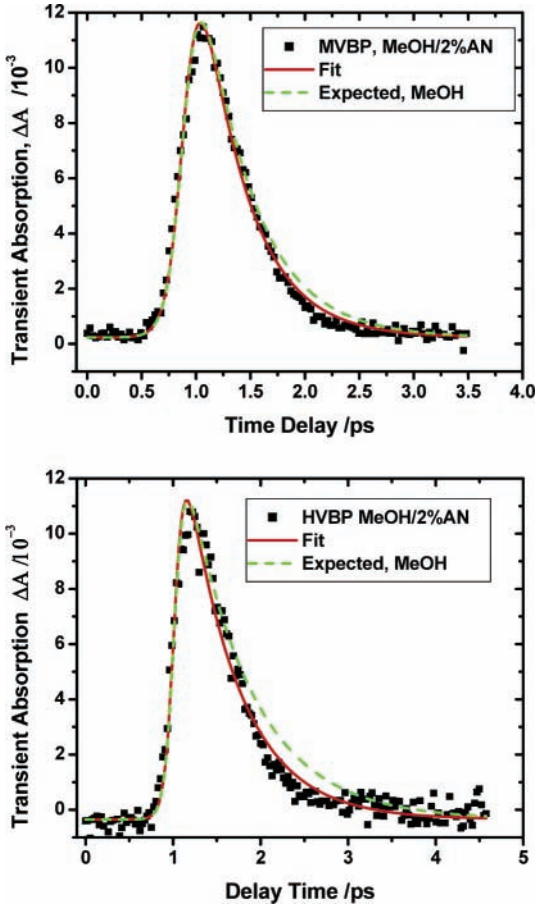

Figure 5. Transient absorption kinetics of MVBP and HVBP in the solvent mixture MeOH/2% AN. The solid curve (red) is a fitted single exponential of 425 (MVBP) and 605 fs (HVBP). The pump wavelength is 490 nm, and probe wavelengths for MVBP and HVBP are 620 and 630 nm, respectively. For comparison, the curve (green) is a computed plot of the expected decay trace in pure methanol using the same excitation pulse as the other signals and the pure MeOH decays of 470 (MVBP) and 730 (HVBP) fs.

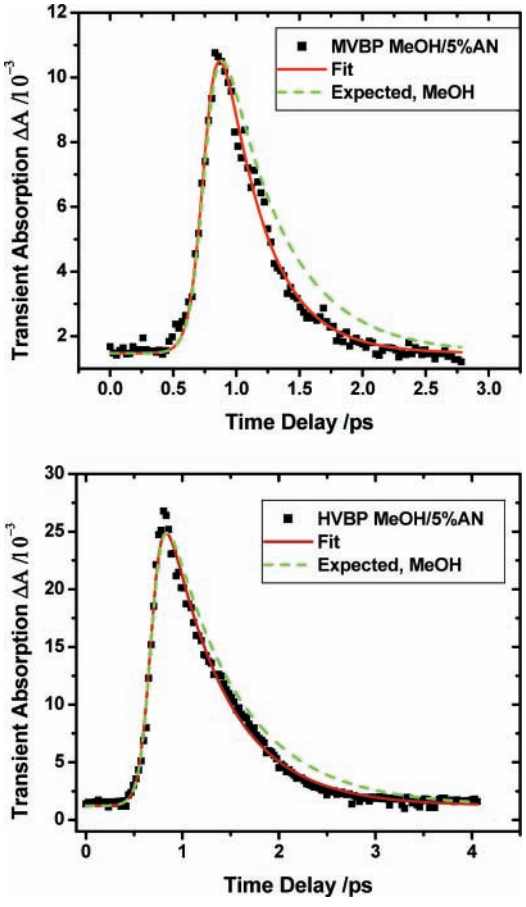

Figure 6. Transient absorption kinetics of MVBP and HVBP in the solvent mixture MeOH/5% AN. The solid curve (red) is a fitted single exponential of 335 (MVBP) and 610 fs (HVBP). The pump wavelength is 490 nm, and the probe wavelengths for MVBP and HVBP is 620 and 630 nm, respectively. For comparison, the curve (green) is a computed plot of the expected decay trace in pure methanol using the same excitation pulse as the other signals and the MeOH decays of 470 (MVBP) and 730 (HVBP) fs.

support the adiabatic model for ET. In addition, we examine the solvent polarity effects on ET rates from changes in energy levels to consider how much this contributes to the observed ET decays. We use a simple ET model with parameters from our earlier work to discuss this latter point, and in later sections we discuss more complete models of solvent relaxation and crossover from nonadiabatic ET to adiabatic ET rates.

B. Solvent Effects on CT Absorption Spectra. The charge-transfer absorption spectra have slightly different peak locations in different solvents, and these shifts can indicate how solvent polarity is stabilizing the CT optical transition. Changes in state energies can lead to different energy gaps and ET rates. The interpretation of ET rates requires a separation of solvent relaxation effects from solvent changes in the state energies. Our prior work in pure MeOH indicated that HVBP has unique solvent dynamic effects on ET compared with MVBP complexes, so we will first examine the MVBP charge-transfer spectra to understand solvent trends. Since our goal is to identify if ET rates are affected by energy level changes, we are making an assumption that energy level changes associated with these small spectral shifts are fully contributing to rate changes so that we can place an approximate upper bound on this contribution to the observed ET rates.

The polar solvation properties of solvents[33] are characterized with the static dielectric constant, ϵ, the solvatochromic polarity, π^*, and the molecular dipole moment in Debye, μ. The values of the (ϵ, π^*, μ) parameters for our solvents are as follows: MeOH (32.7, 0.60, 1.7), AN (35.9, 0.66, 3.53), EtOH (24.6, 0.54, 1.66), and EG (37.3, 0.92, 2.31). For our complexes we expect the solvatochromic parameter to be relevant since charges are delocalized onto the aromatic systems in the radical pair and initial state. In addition, the phenol group of BP and the positive charges in the viologen suggest that the other measures of polar solvation are also appropriate. We tabulate the shifts in charge-transfer peak position in Table 1. For both HVBP and MVBP we note that EG has the largest blue shift for the peak. EG is quite likely more stabilizing than MeOH due to the larger π^* value and slightly larger dielectric constant. This implies that the ground state is more polar than the excited state in these complexes and that for EG there is a larger energy gap than for MeOH.

More subtle trends are expected for the MeOH mixtures with AN at 5, 10, 20 vol %. While a nonprotic solvent like AN will cause other disruptions to solvent hydrogen bonding, we expect that the progressive shift to higher energy peak absorbance in Table 1 is due to the larger dielectric constant and π^* for AN. For EtOH the 10 and 20 vol % cases actually make a slight red shift to lower energy, which could be consistent with the lower dielectric constant and smaller π^* value. The basic conclusion for MVBP is that this complex is showing small wavelength

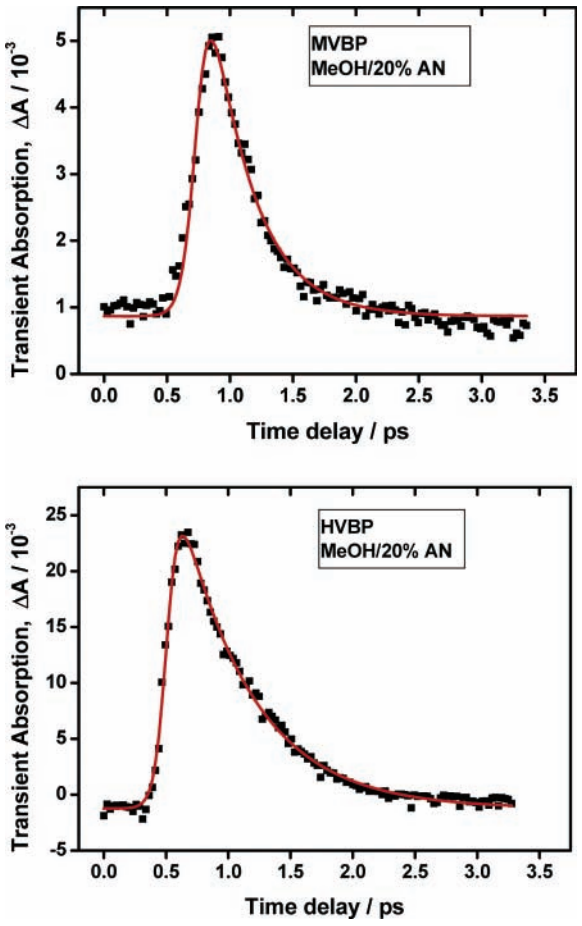

Figure 7. Transient absorption kinetics of MVBP and HVBP in the solvent mixture MeOH/20% AN. The solid curve (red) is a fitted single exponential of 330 (MVBP) and 550 fs (HVBP). The pump and probe wavelengths are 490 and 600 nm, respectively.

shifts consistent with polarity affecting the ground state more than the excited state, so a blue shift occurs in more polar solvent.

For HVBP we see that EG is the best solvent with a peak location identical to MVBP, which suggests that *these two complexes have their electronic systems well solvated with little effect of the HVBP heptyl group*. However, in MeOH the peak location for HVBP shifts further to the red than does MVBP. This suggests that MeOH is not solvating the HVBP complex as well as the MVBP complex. If so, then MeOH and its solvent mixtures can have effects from the heptyl solvation that are not present in MVBP. Table 1 shows that EtOH mixtures of HVBP are slightly more stable than pure MeOH, which is the opposite of MVBP and likely due to changes in heptyl group solvation being more important than average solvent polarity of the mixture. The importance of the heptyl group will be much more obvious in the later discussion of ET decay times.

In summary, the charge-transfer spectra suggest that there are small polarity effects that follow solvent polarity trends for MVBP and less so for HVBP. These spectral shifts can be used to estimate the effect of energy level shifts on ET rates.

C. Electron-Transfer Rates, Solvent Energy Shifts, and Solvent Relaxation. The return electron-transfer decay times are given in Table 2. One important result is that MVBP and HVBP have the same ET rate in EG solvent. This suggests that in EG there is no unusual involvement of the heptyl group. Therefore, this slower relaxing solvent allows the ET to behave according to the energy gap and bulk solvent relaxation effects with no special role of the heptyl group. *Finding such a solvent supports the conclusion in our original work that these two complexes should have the same ET rate if solvent effects were similar*. For MVBP in EG the absolute value of the decay time is much larger than in MeOH, and this effect could be due to a solvent relaxation change and/or an energy level change. Therefore, this case is important to model. Much smaller changes in polarity occur for the solvent mixtures, but they have large changes in ET decay rates in some cases. We shall argue that those ET trends support the importance of solvent relaxation changes.

One approach for estimating the effects of solvent polarity on ET rate is to use a simple theoretical calculation of ET rate with realistic experimental parameters and energy level changes from the observed solvent shifts of the CT spectra. The easiest case is to use relative changes in predicted nonadiabatic ET rates with our prior estimates of ET parameters, which are shown in Table 3. A typical expression[1,2] for k_{NA} is given as

$$k_{NA} = \frac{2\pi}{\hbar} V^2 (4\pi\lambda_t k_B T)^{-1/2} \exp\left[-\frac{(\lambda_t + \Delta G)^2}{4\lambda_t k_B T}\right] \quad (1)$$

In this modified classical form we have $\lambda_t = \lambda_S + \lambda_V$, where solvent and vibrational reorganization energies are given by λ_S and λ_V, respectively, and ΔG is the free energy change and V is the coupling matrix element. The activation free energy inside the exponential is given by the well-known parabolic form of Marcus[34] where G^* is given by

$$G^* = \left[\frac{(\lambda_t + \Delta G)^2}{4\lambda_t}\right] \quad (2)$$

We see from this equation that polarity changes enter in both the solvent reorganization parameter and the energy gap through ΔG. The energy gap effects dominate for changes between MeOH and EG, where an estimate of the solvent reorganization correction only increases the rate by ~3% for EG. Therefore, we only use shifts in the energy gap to estimate polarity effects on ET decay times.

Since MVBP had polarity shifts in the CT spectra that seem to follow expectations due to polarity trends, we can compare its ET rate predictions in MeOH and EG with the data. As we discuss in the next section, the exact balance between solvent reorganization and vibrational reorganization energies is not known, but a self-consistent set of ET parameters is possible for the estimated solvent reorganization value of 6162 cm^{-1} and a trial assumption of zero activation free energy. From Table 1 the shift in CT spectra between EG and MeOH is computed to be 589 cm^{-1}. With this value the predicted upper bound for the decay time ratio is $\tau_{EG}/\tau_{MeOH} = 1.40$, which is to be compared with an observed ratio in Table 2 of 1.91. This suggests that polarity changes are part of the ET rate effect with solvent relaxation adding a factor of 1.36. Additional confirmation of important solvent relaxation effects is found in the mixture data. If we examine ET decays for MVBP in MeOH for 5%, 10%, and 20% AN, the decays are nearly constant at 330 fs vs pure MeOH at 470 fs. The constant decay is not what is expected from the polarity trend of Table 1 since the ET decay did not increase as the percent AN increased, which is the expectation for an increasing energy gap. For the 20% AN case we use the 169 cm^{-1} CT band shift to predict $\tau_{EG}/\tau_{Mix} = 1.09$, where the data show 0.70 for the ratio. This is an opposite effect from polarity as is true for all AN mixtures. However, since AN has faster dielectric relaxation times (see below) than MeOH

TABLE 2: Decay Times for Electron Transfer[a]

solvent[b]	MVBP τ (fs)	error (fs)	τ/τ_{MeOH}	ratio error	τ/τ_{EG}	HVBP τ (fs)	error (fs)	τ/τ_{MeOH}	ratio error	τ/τ_{EG}
MeOH	470	20	1.00		0.52	730	30	1.00		0.82
EG	900	35	1.91	0.06	1.00	885	35	1.21	0.06	1.00
MeOH/AN(2%)	425	20	0.90	0.06	0.47	605	25	0.83	0.06	0.68
MeOH/AN(5%)	335	20	0.71	0.07	0.37	610	25	0.84	0.06	0.69
MeOH/AN(10%)	325	20	0.69	0.07	0.36	540	20	0.74	0.06	0.61
MeOH/AN(20%)	330	20	0.70	0.07	0.37	550	20	0.75	0.05	0.62
MeOH/EtOH(2%)	405	20	0.86	0.07	0.45					
MeOH/EtOH(5%)	390	20	0.83	0.07	0.43	775	30	1.06	0.06	0.88
MeOH/EtOH(10%)						685	30	0.94	0.06	0.77
MeOH/EtOH(20%)						700	30	0.96	0.06	0.79

[a] The decay time error is estimated from error estimates in the fitting procedure and averages over multiple experiments. The ratio errors are for the column to the left, τ/τ_{MeOH}. τ/τ_{EG} is for reference in the discussion. [b] Solvents are as follows: methanol, MeOH; ethylene glycol, EG; acetonitrile, AN; ethanol, EtOH.

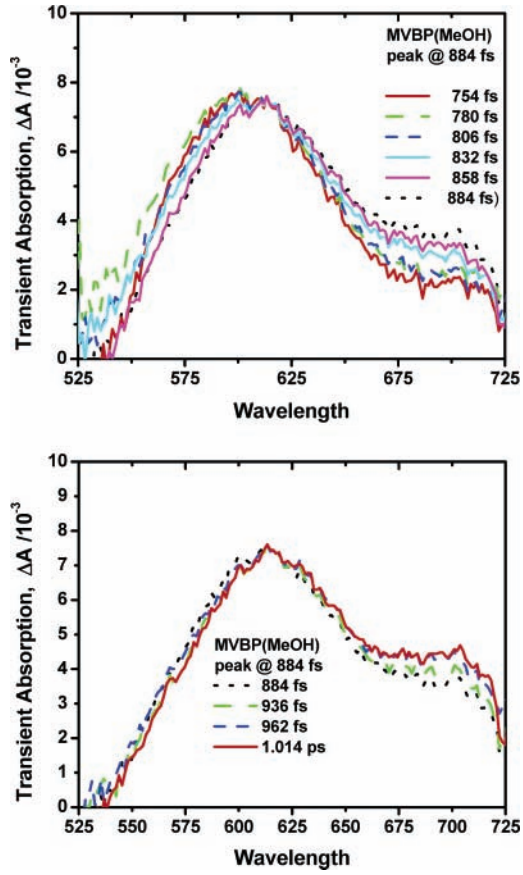

Figure 8. Transient absorption of MVBP in MeOH for a series of time delays. The time scale is arbitrary, and the peak absorption is the reference point to compare with kinetic decays.

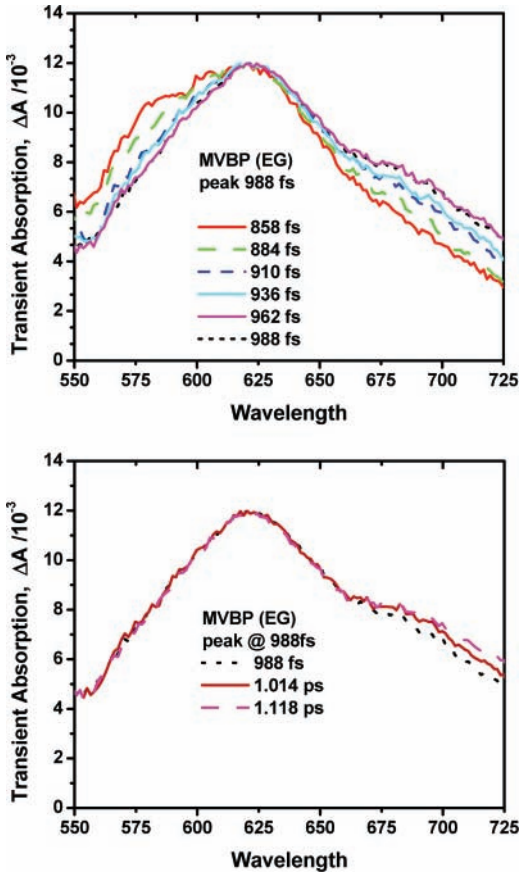

Figure 9. Transient absorption of MVBP in ethylene glycol at a series of delay times. The time scale is arbitrary, and the peak absorption is the reference point to compare with kinetic decays.

and is not hydrogen bonding, one might argue for compensation of a small polarity effect with a large solvent relaxation effect that leaves the decay time in 5%, 10%, and 20% AN mixtures at a constant value. The 2% AN data shows a significant change of ET decay to 425 fs, which is not likely to be from polarity but from disruption effects of AN on the MeOH solvation structure. This disruption idea is supported with the EtOH data, where 2% and 5% mixtures also slightly lower the ET decay to ~400 fs, even though EtOH has slower relaxation times than MeOH and is a hydrogen-bonding solvent with a polarity spectral shift that implies lengthening the decay time. Therefore, it is quite likely that in mixtures the energy level changes in MVBP have minor effects on ET rates in comparison with solvent relaxation effects. Even the large change in ET decay between EG and MeOH has a large solvent relaxation component of ~40%.

For HVBP in EG the ET decay is about the same as MVBP, and for MeOH the HVBP has a much larger decay time than MVBP. When considered with the spectral shift data, this suggests that in MeOH the heptyl group is perturbing the solvation. It could be that the heptyl group average position in MeOH is closer to the aromatic systems or that the local solvation structure of MeOH must change due to the heptyl perturbation. The CT absorption shift for HVBP between EG and MeOH is 1120 cm^{-1}, which predicts a $\tau_{EG}/\tau_{MeOH} = 2.05$ rather than the observed ratio of 1.21. This suggests that the heptyl group effect is much different than expected from solvation energy since the MeOH ET decay time is much longer than expected by solvent polarity effects. For the case of 20% AN the CT absorption shift predicts $\tau_{Mix}/\tau_{MeOH} = 1.52$ while the data have a ratio of 0.75, a divergence in the opposite direction of polarity. *Since the spectral shifts for MeOH/AN*

TABLE 3: Summary of Electron-Transfer Parameters Derived from Absorption and Raman Spectra[21]

parameter	MVBP	HVBP
$\epsilon/M^{-1}\,cm^{-1}$	40	40
$\bar{\omega}/cm^{-1}$ [a]	21300	21275
$\delta\bar{\omega}/cm^{-1}$ [a]	5770	6435
$r/Å$ [b]	4.0	4.0
V/cm^{-1} [c]	361	381
Δ/cm^{-1} [d]	1598	
λ_S/cm^{-1} [e]	6162	
$R/Å$ [f]	6.02	

[a] Fit to absorption spectra. [b] Distance between donor and acceptor sites. [c] $V = 0.0206r^{-1}(\epsilon\bar{\omega}\delta\bar{\omega})^{1/2}$. [d] Equation 7. [e] λ_{CM} in previous paper. [f] From 0.001 esu/bohr^3 electron density contour calculated at the B3LYP/6-31G(d) level.

mixtures increase the energy gap, which should correlate with a longer decay time, the observed reduction of the decay time cannot be dominated by energy level shifts. This suggests that the MeOH solvent structure is perturbed by the heptyl group and that by adding AN or EtOH this perturbation is changed without ever achieving a solvent structure similar to MVBP (i.e., a similar ET decay time). The AN mixtures of 2% and 5% have similar decays for HVBP and are 0.83 times the MeOH decay. For HVBP in solvent mixtures with 5%, 10%, and 20% EtOH we expect progressive lifetime changes consistent with solvation energies rather than the approximately constant decay time similar to pure MeOH. This suggests that the EtOH perturbation is insufficient to significantly change the solvent structure.

One can conclude for HVBP that the ET decay rate of HVBP in MeOH and its mixtures is dependent on the relaxation behavior of the perturbed solvent structure created by the heptyl group. Since the ET decay is longer for HVBP in MeOH than MVBP in MeOH and is not greatly different from EG, we infer that the longer relaxation of MeOH for HVBP is due to heptyl group perturbation. This was the hypothesis of our prior work, but the solvent effects shown here give a much better insight into the effect. This is also supported by calculations (see below) that suggest MeOH should have much faster solvent relaxation than EG.

In summary, the ET decays show large effects of solvent relaxation in MeOH and MeOH mixtures for both MVBP and HVBP. The large ET decay difference between EG and MeOH for MVBP and identical ET decays of MVBP and HVBP in EG demonstrate that EG solutions have similar local and bulk solvation in both complexes. However, MeOH and MeOH mixtures have large solvent relaxation effects for both complexes, and there is unusual solvation of HVBP that lengthens the solvent relaxation time compared with MVBP. Quantitative solvent relaxation models will be discussed in the next section.

V. Discussion of Solvent Relaxation Models and Data

A. Overview. For ET processes there have been many theoretical studies of how solvent relaxation effects are manifested in the observed rates. There are a group of theoretical models that allow a continuous evolution from nonadiabatic ET rates to purely solvent-controlled adiabatic rate models as the solvent relaxation time increases. These models compute an adiabaticity parameter that has been useful for interpreting some types of ET processes. However, failure of the model is often seen for nonadiabatic ET cases where the rates are thought to involve larger components of vibrational reorganization energy, as found in the inverted region of electron transfer. Continuous crossover between adiabatic and nonadiabatic ET rates has little experimental confirmation. The experimental data appears to fall into two cases: one with clear solvent control on longer time scales and the other with pure nonadiabatic rate control and small solvent effects. The experimental difficulty of independently tuning solvent relaxation times without changing energy level positions, coupling matrix elements, local solvation of the solute, and solvent viscosity usually results in limited ability to explore a given ET system. Indeed, even identifying enough system parameters to model an absolute nonadiabatic rate and thereby identify unambiguous solvent relaxation effects is quite difficult.

Therefore, one of the primary goals of this work is to identify how solvent control of ET operates in the ultrafast ET domain. We use experimental solvent parameters and theoretical models to show that solvent control is operating in our particular system. We then compare different models to identify what experimental and theoretical work is needed to fully understand ultrafast ET with solvent control. The following sections first make a brief review of the extensive theoretical and experimental literature in this area before applying those ideas to our data in Section D.

B. Theoretical Models for Solvent Control of ET. A recent review on ET has been published by Bixon and Jortner,[1] and earlier reviews of Marcus and Sutin[34] and Newton[35] are useful general references on ET. The theoretical literature of solvent effects on ET is quite large, and we reference a subset of those articles with connection to ultrafast ET and crossover from nonadiabatic to adiabatic behavior in solvents.[1−9] The initial work of Zusman[6] established the concept of how solvent relaxation could control the rate of an electron-transfer system in the adiabatic limit with an analytical model for the degree of solvent control. This model uses an adiabaticity parameter, g, for describing the crossover between adiabatic and nonadiabatic behaviors, as in eq 3. There have been different versions of the adiabatic parameter, g, in the literature; we give some of these later.

$$k_{ET} = k_{NA}\left[\frac{1}{(1+g)}\right] \tag{3}$$

An ET rate of the generalized Zusman form has been derived with a number of models; for example, recent spin-boson models[36−38] have compared their numerical results with a Zusman-type analytical model similar to Garg et al.[4] This analytical rate constant uses a solvent relaxation time, $1/\omega_c$, which also has been converted to a relaxation frequency $\omega_r = \omega_c/2$ in a solvent model[36] with an ohmic spectral distribution and cutoff frequency ω_c. The experimental description of solvent effects often uses a simple Debye solvent model, where the energetics of solvent relaxation is described by a longitudinal relaxation time,τ_L, where $\tau_L = (\epsilon_\infty/\epsilon_S)\tau_D$ with static dielectric constant, ϵ_S, and infinite frequency dielectric constant, ϵ_∞, modifying the Debye relaxation time,τ_D. A rate constant form similar to Zusman that also uses τ_L similarly was derived by Rips and Jortner,[5] with a form as given by eqs 1−3 with an adiabatic parameter, g_{RJ} as

$$g_{RJ} = \frac{4\pi V^2 \tau_L}{\hbar\lambda_S} \tag{4}$$

Other treatments have given similar crossover equations but with a different form of the adiabaticity parameter. A model by Sparpaglione and Mukamel[8,9] uses a time correlation function of general form that allows computing a relaxation time, $\tau(q)$, as

$$\tau(q) \equiv \exp\left(\frac{-q^2}{2}\right)\int_0^\infty \mathrm{d}t\left\{\frac{1}{\sqrt{1-M^2(t)}}\exp\left[\frac{q^2M(t)}{1+M(t)}\right]-1\right\} \tag{5}$$

where $M(t)$ is the solvation correlation function and the activation energy parameter, q, is given by

$$q^2 = \frac{2G^*}{k_\mathrm{B}T} \tag{6}$$

As we discuss below, the solvation correlation function may assume an arbitrary functional form, allowing multiple relaxation modes to enter the calculation rather than a single dielectric relaxation time. Their work predicts a crossover equation of similar form to Zusman but with a different adiabaticity factor, g_{SPM}, that includes temperature, T, because of its use of spectral line shapes. In eq 7 we show the static limit of a line shape model[8,9] that gives the solute−solvent coupling, Δ, in terms of solvent reorganization energy.

$$\Delta^2 = 2\lambda_\mathrm{S}k_\mathrm{B}T \tag{7}$$

We also assumed that ground-state activation is negligible, so that only one relaxation time is operative, which we write without a subscript. In our prior study of ET in these complexes we discussed the solvent relaxation model used in the work of Sparpaglione and Mukamel (SPM),[8,9] and in this work we will extend our discussion to compare with ET decay predications of other models. For the predicted rate of the form of eq 3 the SPM model has an adiabaticity parameter

$$g_{\mathrm{SPM}} = \left(\frac{2\pi V^2}{\hbar}\right)\left(\frac{1}{(4\pi\lambda_\mathrm{S}k_\mathrm{B}T)^{1/2}}\right)\tau(q) \tag{8}$$

All of these models[4−6,8,9] do not consider the internal vibrational degrees of freedom, whose reorganization energy, λ_V, can play a major role in defining the ET rate for the activationless ($-\Delta G = \lambda$) and inverted ($-\Delta G > \lambda$) regions of ET. The simplest modification that includes this parameter was given in eq 1. With this modification the adiabaticity factor, g, still would use λ_S for the relevant solvent reorganization energy. This modified classical form is most useful for very small activation energies. Semiclassical models[1] that explicitly use high-frequency vibrational coordinates for the ET system predict much faster ET rates for inverted region ET than the modified classical rate expression. The vibrational reorganization contribution to ET has little time dependence in the ideal case, and therefore, one might expect that the adiabaticity factor should depend on the amount of vibrational reorganization versus solvent reorganization. This was considered by Sumi and Marcus,[7] and they showed how vibrational reorganization could affect the adiabaticity in a classical ET rate expression of eq 1. They give equations (see eq 8.3′) to compute a numerical factor, F, which multiplies τ_L, to form a correction to the nonadiabatic decay time. For this treatment the adiabaticity parameter is

$$g_{\mathrm{SM}} = k_{\mathrm{NA}}F\tau_\mathrm{L} \tag{9}$$

and the electron-transfer decay is given in eq 10 by $1/k_{\mathrm{SM}}$.

$$\tau_{\mathrm{SM}} = \frac{1}{k_{\mathrm{SM}}} = \frac{1}{k_{\mathrm{NA}}} + F\tau_\mathrm{L} \tag{10}$$

Their classical treatment is best used near the activationless region. For highly inverted regions a simple modification of their model that adds one vibrational high frequency has been used for betaine interpretations in the inverted region of ET.[26]

In later sections we discuss these models in the context of our experimental data.

C. Solvent Relaxation Times and Solvent Correlation Functions. A method of defining solvent correlation functions uses excited-state fluorescence spectral shifts versus time as a measure of energetic stabilization by solvent relaxation. Such data has been extensively compiled for many solvents by Horng et al.[39] While one might suspect that each probe molecule might have unique relaxation character that is a convolution of molecule and solvent, a number of studies, including optical frequency dielectric relaxation,[40] support the suggestion that coumarin 153 provides a measure of the bulk solvent correlation function. This correspondence is still open to further study, but for fast relaxing molecules such as acetonitrile there is reasonable agreement with a variety of methods and theory.[41] Table 4 shows some of the results for solvents of interest in this work. We note that the fastest component for MeOH and EtOH was assigned a value of 0.03 ps by Horng et al.,[39] which is shorter than in some recent reports; we give three different sets of values for methanol[24,39,42] and two for acetonitrile.[24,39] The theoretical modeling of alcohols[43] and acetonitrile[41] has shown consistency with most of the experimental work on dye relaxation and dielectric measurements, although one methanol result[44] appears to disagree with these models due to its large amplitude of fast component.

We next examine the dependence of the relaxation time using a full correlation model[8,9] that was discussed above. We use the solvent correlation times to define $M(t)$ in eq 5 and compute the effective relaxation times in Table 4 and Figure 10. In Table 4 we report an "average" relaxation time, τ_0, obtained by inverting a weighted average of the relaxation rates. This is often used to characterize the net effect of a multicomponent relaxation. The time correlation method gives a relaxation time that depends on exothermicity, and we report two such times for values of τ at $q = 0$ and 1 in Table 4. Plots of such times as a function of q are given in our prior work,[21] and a more extensive set is shown in Figure 10. In Figure 10 we show MeOH-v1, AN-v1, and EG for Horng et al.[39] and also MeOH-v3 from Bingemann et al.[42] and a mixture of MeOH-v3 with 20% AN-v1. As can be seen in Table 4, MeOH-v2 is similar to MeOH-v3, so it is not plotted in Figure 10; however, MeOH-v2 is a more recent result from the same group, so it might be the best result. The time correlation model suggests that there is no fixed value of relaxation time applicable to all ET cases and that relaxation time is not easily associated with a single component of the correlation function or τ_0, the average relaxation time. As we discuss below, our ET is likely to have small activation energy, so that smaller values of q (<1.5) in Figure 10 are most relevant. This method also allows adding components to approximate a mixture, and one such example is in Table 4 and Figure 10, where we model 20% AN in MeOH to see what effects might occur if it behaved according to a simple proportionality. Interestingly, the mixture predictions for τ ($q = 0$) show a 29% drop in relaxation time, while there is a 17% drop inferred from the simple weighted average, τ_0; this may support the observed large drop in decay time for AN mixtures in Table 2.

While relaxation times for our solvent mixtures are not available, far-infrared spectra and molecular simulations have been done for methanol with acetonitrile mixtures[45−47] at AN volume fractions of 0.1, 0.25, 0.5, and 0.75. The spectra show a red shifting and broadening of the high-frequency absorption

TABLE 4: Time Correlation Functions for Solvents

solvent[a]	τ_1	A_1	τ_2	A_2	τ_3	A_3	τ_4	A_4	τ_5	A_5	τ_0[c]	$\tau\ (q=0)$[d]	$\tau\ (q=1.0)$[d]
MeOH-v1[39]	0.03[b]	0.101	0.28	0.34	3.2	0.298	15.3	0.061			0.21	0.362	0.61
MeOH-v2[24]	0.1	0.3	0.97	0.34	11	0.36					0.30	0.356	0.598
MeOH-v3[42]	0.07	0.3	0.8	0.3	6.4	0.4					0.21	0.303	0.537
EtOH[39]	0.03[b]	0.085	0.39	0.23	5.0 3	0.182	29.6	0.502			0.29	0.612	0.900
EG[39]	0.187	0.307	4.98	0.255	32	0.437					0.59	0.608	0.889
AN-v1[39]	0.089	0.686	0.63	0.314							0.12	0.094	0.198
AN-v3[24]	0.07	0.67	0.6	0.33							0.10	0.079	0.18
80%MeOH/20% AN[e]	0.07	0.24	0.8	0.24	6.4	0.32	0.089	0.1372	0.63	0.0628	0.18	0.235	0.448

[a] Solvents are as follows: methanol, MeOH; ethylene glycol, EG; acetonitrile, AN; ethanol, EtOH. The individual components are expe. [b] The 0.03 ps component is an estimate and not resolved in this group's report.[39] [c] The τ_0 parameter is defined from the components. $1/\tau_0 = \sum_i A_i/\tau_i$. [d] τ $(q = 0)$ and τ $(q = 1.0)$ are computed from a solvent model at a specific activation energy parameter, q. [e] The mixture used MeOH-v3 from Bingemann et al.[42] and AN-v1 from Horng et al.[39]

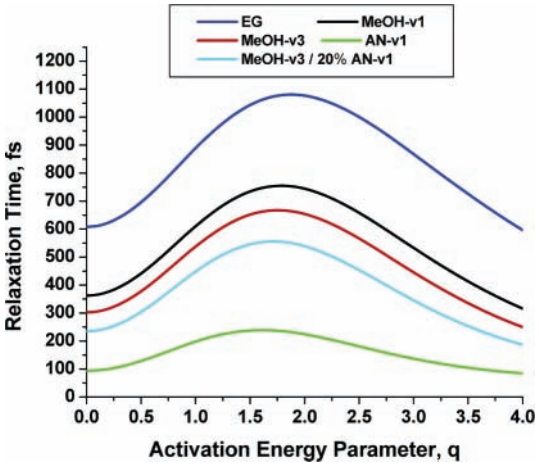

Figure 10. Relaxation times from solvent correlation functions versus activation energy parameter, q.

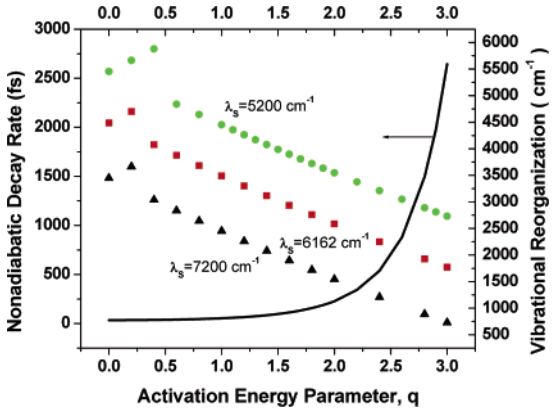

Figure 11. Computed nonadiabatic electron-transfer decay (left, black line) versus activation energy parameter, q. Computed vibrational reorganization energy for different solvent reorganization energies, λ_S.

peak at 669 cm^{-1}, and these data and modeling are interpreted as being due to breaking up the hydrogen bonding in the methanol chains and network by acetonitrile. Other experiments confirm this idea,[48] but thus far no relaxation times are available for such mixtures.

D. Models for Electron Transfer in Viologen/Biphenyl Charge-Transfer Complexes. The physical picture of ET in our systems is an optical direct excitation of an electron to a charge-transfer state, where the electron is associated with specific molecules and back ET returns the ground state. We are monitoring the radical state of MV or HV in the MVBP or HVBP pair. Our previous publication discussed the ET model parameters for the charge-transfer complexes MVBP and HVBP. These parameters are reproduced in Table 3 for convenience since we use them in our discussion. The charge-transfer band was used to infer a coupling matrix element, V, of 361 cm^{-1} for MVBP.[21] This value is 5−10 times larger than a pure weak coupling case at $k_BT \approx 207$ cm^{-1}, but coupling of this size is often considered consistent with a nonadiabatic ET model. The structure of the complex is reasonably stable, and our computer models for gas-phase structure suggest it is not likely to be greatly heterogeneous.[21] Both MVBP and HVBP have similar oscillator strengths, independent of the hydrogen-bonding polar solvents (MeOH and EG), which implies that the complex structure is weakly dependent on these solvents. Since the complex is not soluble in a large number of solvents (at high concentrations where we seek to do experiments), there are probably specific interactions in the first solvent shell that change the interface to the bulk structure. Theory[31] suggests that the radical cation of the viologens can assume a planar configuration of the two aromatic rings so that some intramolecular coordinate motion may be involved in the ET coordinate.

From Figures 8 and 9 we find small changes in the transient spectrum in the first 100−150 fs before the peak (early in the rise time of kinetic traces), which suggests that any such motion is faster than 100 fs. Unlike some of the strongly coupled intramolecular ET cases discussed above, we can approximate this system with a simple ET reaction coordinate that is described by two offset parabolas with an exothermicity similar to the total reorganization energy. The data supports treating this as a nonadiabatic ET model with small or zero effective barrier, although not all parameters have been defined for solvent and vibrational reorganization energy and exothermicity of the reaction. However, for optically excited ET there are constraints on the sum of free energy and total reorganization energy that allow us to compute a range of parameters for comparison with experiment, and this range will guide our conclusions.

The constraint offered by the optical excited charge transfer allows us to use a modified classical model of eq 1 to compute a nonadiabatic ET rate constant with a total reorganization equal to vibrational plus solvent reorganization energy. We computed nonadiabatic ET rates by systematically varying ΔG^* for three values of λ_S at 5200, 6162, and 7200 cm^{-1} to infer the corresponding vibrational reorganization energy and exothermicity, ΔG, of the ET. For convenience with comparing to one model[8,9] we use the parameter $q^2 = 2\Delta G^*/k_BT$ (in our prior work q had a subscript, q_a). The optical excited state at frequency $\omega = 21\,300$ cm^{-1} is defined by the exothermicity and total reorganization energy, $\omega = \Delta G + \lambda_t$. For any given q value we solve for the other parameters, and Figure 11 plots the activation energy parameter q versus the nonadiabatic ET decay time (left axis) and the resulting vibrational reorganization energy (right axis) for these three values of λ_S. The nonadiabatic model of eq 1, a modified classical model, yields results for very low activation energy that are similar to a quantum model.

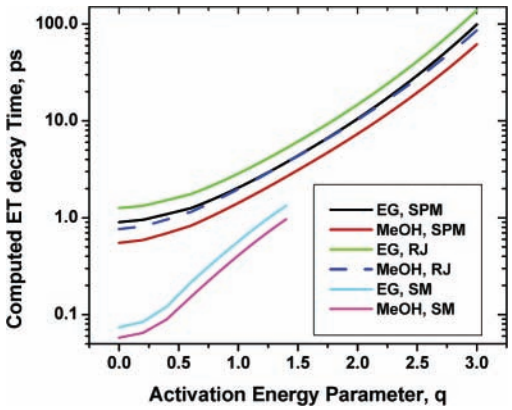

Figure 12. Model predictions of electron-transfer decay times versus activation energy parameter, q.

We note that for zero activation energy the ET decay time is 34 fs, and it lengthens to 53.5 fs for $q = 1.0$ ($\Delta G^* = 103$ cm^{-1}) and to 228 fs for $q = 2.0$ ($\Delta G^* = 414$ cm^{-1}). The times for $q = 0$ and 1 are much smaller than the observed experimental times. Experimental values for λ_V can be used to narrow the range of estimates for an intrinsic nonadiabatic ET rate. Some estimates[49] for the MV part of the charge-transfer pair suggest values in the 4200−5600 cm^{-1} range, so that with some additional contribution from biphenol in MVBP, the value of vibrational reorganization could easily be in the range of 5000−6000 cm^{-1}. Without a resonance Raman study and theoretical confirmation of vibrational frequency changes it is difficult to know if this value is correct, but it is also consistent with solvent reorganization energy in the 5000−6000 cm^{-1} range. From the plot in Figure 11 one sees that small activation energy and λ_S values near our trial values of 5200 and 6162 cm^{-1} are most likely.

The different models of crossover between nonadiabatic and adiabatic ET can be compared to see if their predictions are consistent with a solvent relaxation modification of nonadiabatic ET. The theoretical crossover models predict final ET decays through an adiabaticity parameter (see eqs 3, 4, 8, and 9). Recall from our prior discussion that the SM model attempts to incorporate a possible effect from a large component of vibrational reorganization energy. We use the case of $\lambda_S = 5200$ cm^{-1} to plot the predictions of Sparpaglione and Mukamel[8,9] (τ_{SPM}), Rips and Jortner[5] (τ_{RJ}), and Sumi and Marcus[7] (τ_{SM}) versus activation energy in Figure 12. The choice of $\lambda_S = 6162$ cm^{-1} is not very different. We use the models of relaxation time for MeOH-v1 and EG in Table 4. The final relaxation time depends on q, as calculated by the SPM model. Some representative values of the parameters and resultant predictions are given in Table 5. Table 5 assumes the energy gap is identical for MeOH and EG, and the best solvent for absolute experimental comparison is EG. We report sufficient significant figures to allow easier duplication of model calculations, but clearly the experimental accuracy does not justify this precision. The predictions of SPM[8,9] and RJ[5] are different because of the different solvent reorganization dependence in the two models, but both models are only consistent with the EG data for very small activation energies ($q \approx 0$). The result for the SM[7] model is somewhat different in that very small activation energies also give small values of the multiplying factor, F (see Table 5). The value of F changes rapidly from $q = 0$ to 1.2, and in this model a factor near unity is required to give agreement with the EG experimental result. For the calculations at $q = 1.2$ we find that the SM model requires $\lambda_V = 4262$ cm^{-1} and a ratio $\lambda_V/\lambda_S = 0.82$, which is consistent with our reorganization estimates.

The models establish adiabatic solvent control as a likely mechanism for this ET reaction. The need for using a range of parameters does not allow choosing between models. If we use EG versus MeOH solvent as a point for comparing with experiment, then for the SPM model at $q = 0$ we find values for the ET decay EG:MeOH as 902: 552 versus the experimental value of 900:470. The RJ model predicts values of 1257: 763 where both models have MeOH at about 61% of the EG value rather than the experimental fraction of 52%. These comparisons do not correct for the energy gap shift, but we gave estimates above that predicted that the 470 fs decay of MeOH could be 1.40 times larger (660 fs), which is 73% of the EG value versus the computed 61%. With the energy level correction the level of agreement is reasonable. However, the SPM and RJ models do not correct for the vibrational reorganization component. The SM model corrects for this effect and predicts the ratio of ET decay times EG:MeOH for $q = 1.2$ as 890:641 where MeOH is at 72% of the EG value. This is in better agreement with experiment, but it is not clear if this difference is significant without precise values for the vibrational and solvent reorganization energies.

All of the models are in reasonable agreement when we consider the complexity of solvent effects in the experiments, which were discussed previously. Many of these effects are found in any ET system in hydrogen-bonding solvents. The first solvent shell in our system requires hydrogen bonding to the complex for solubility, and EG seems to be a better solvent than MeOH since HVBP and MVBP had similar ET behavior. The EG case probably allows full extension of the heptyl group

TABLE 5: Electron-Transfer Decay Times for Models[a]

					TCF	TCF	EG	EG	MeOH	Me OH	EG	EG	MeOH	MeOH		EG	MeOH
q	G^* (cm^{-1})	τ_{NA} (fs)	λ_V (cm^{-1})	Δ_G (cm^{-1})	τ_{MeOH} (fs)	τ_{EG} (fs)	g_{SPM}	τ_{SPM} (fs)	g_{SPM}	τ_{SPM} (fs)	g_{RJ}	τ_{RJ} (fs)	g_{RJ}	τ_{RJ} (fs)	F_{SM}	τ_{SM} (fs)	τ_{SM} (fs)
0	0	34.1	5454	−10 646	362.4	607.6	25.5	902	15.2	552	35.8	1257	21.4	763	0.066	74	58
0.4	16.5	37.7	5878	−10 222	414.5	665.8	27.9	1089	17.4	693	39.3	1519	24.5	960	0.125	121	90
0.8	66.2	45.2	4643	−11 457	540.4	808.3	33.9	1576	22.6	1069	47.7	2201	31.9	1486	0.381	353	251
1	103.4	53.5	4451	−11 649	609.6	888.6	37.2	2045	25.5	1420	52.4	2858	36.0	1978	0.581	570	408
1.2	149.2	66.1	4262	−11 838	671.1	962	40.3	2730	28.1	1925	56.8	3818	39.6	2683	0.856	890	641
1.6	265	113.5	3897	−12 203	746.2	1060.6	44.4	5157	31.3	3662	62.6	7216	44.0	5110			
2	414	228	3547	−12 553	744.2	1077	45.1	10 517	31.2	7338	63.5	14 716	43.9	10 239			
2.4	596	539	3211	−12 889	680.2	1022	42.8	23620	28.5	15 901	60.3	33 040	40.1	22 170			
2.8	811.6	1497	2888	−13 212	584.3	924.3	38.7	59473	24.5	38 147	54.5	83 134	34.5	53 104			
3	931.4	2644	2732	−13 368	533.1	868	36.4	98804	22.3	61 703	51.2	13 8049	31.5	85 806			

[a] Model with $V = 361$ cm^{-1}, $\lambda_S = 5200$ cm^{-1} for all solvents. See Table 3 for other parameters. TCF is from the model of SPM[8,9] with solvent data from Horng et al.[39] F_{SM} is from the model of Sumi and Marcus.[7] Model abbreviations are as follows: RJ,[5] SPM,[8,9] and SM.[7] Solvents are as follows: methanol, MeOH; ethylene glycol, EG.

and much less perturbation of the first solvent shell and nearby solvent configurations. We might expect EG to have similar relaxation properties near and far from the MVBP since the hydrogen-bonding character exists on both ends of the molecule, which means that the first solvent shell is more similar to bulk. The comparison of ET behavior of MVBP and HVBP is then a good test of solvation uniformity. However, alcohols such as MeOH are more heterogeneous, and MeOH has opposed hydrophobic and hydrogen-bonding ends, which can easily require a first solvent layer that distorts the molecular transition to bulk. For MVBP and HVBP in MeOH the results were quite different, 470 and 730 fs, respectively. This result and the effects of adding even very small amounts of AN suggested that MeOH has some unusual solvent order around HVBP and MVBP, which can be perturbed easily. The effect of 5% AN on MVBP where ET decay was reduced to 71% of pure MeOH also suggests that perturbation of local solvent structure is more important than could be inferred by average effects of dielectric constant. The richness of MeOH behavior suggests that it is not easy to model its ET rates by a simple bulk solvent model, and it may take molecular dynamics models with accurate local solvation to explain this solvent in ET cases where local solvation structure is important. As we have done here, using solvent correlation functions derived from dye molecules can get close to providing data of relevance to such complex cases. However, ultimately a complete quantum and molecular dynamics model is likely to be necessary for understanding the full solvation shell effect on ET.

VI. Conclusion

These studies demonstrate that ultrafast ET in our viologen charge-transfer complexes has solvent relaxation effects that are consistent with adiabatic crossover models of nonadiabatic ET. Furthermore, by using solvent mixtures and diheptyl viologen to replace dimethyl viologen in the complexes, we demonstrate ET effects that can be associated with the nature of local solvent order. The complex of biphenol with either dimethyl viologen or diheptyl viologen shows identical charge-transfer spectra and ET kinetics in ethylene glycol. However, in methanol and in mixtures having low (2−20%) concentrations of acetonitrile in methanol the ET kinetics show significant perturbations that we associate with perturbations of local solvation. A large difference between MVBP and HVBP complexes in MeOH suggest that a different solvent reorganization time is associated with the heptyl viologen complex. However, for HVBP this solvent coordinate need not involve only bulk solvent reorganization since the volume of the heptyl groups is relatively small compared with the first solvent layers. We used a classical nonadiabatic ET model with several models for adiabatic crossover predictions to discuss the small energy gap effects in this system and approximately model the ET rates derived from adiabatic solvent control of ET.

These charge-transfer systems appear to be good for studying adiabatic solvent effects since they have reasonably well-defined geometry with weak electronic coupling, where the electronic transitions are not dependent on intramolecular motions. For this case, standard nonadiabatic rate constant models can be used to model ultrafast ET rates in the approximately zero-barrier region of ET with crossover adiabatic corrections. The data shown here suggest that more theory incorporating vibrational reorganization effects might be required to understand the crossover to adiabatic behavior. A new theoretical investigation combining elements of the SPM and SM models might be useful for interpreting future experiments.

New experiments on this and related systems are required to fully understand solvent effects on ET. Solvents for these particular CT complexes should emphasize EG and other glycols and examine temperature effects and mixtures chosen to break structure uniformly (mixtures of glycols) or less uniformly (glycols and alcohols) or more dramatically (glycols and dipolar aprotics). Solvent components with strong hydrogen bonding, such as fluoroethanol, might be useful for investigating local solvation effects. Since internal vibrational reorganization contributions to the rate can prevent creating a very wide range of solvent relaxation times, carefully chosen ET systems and mixtures are required to provide the best insight in future work. In our case we had two electronically similar complexes that could reveal unusual local solvent ordering effects. For mixtures, a variety of solvent correlation functions will be needed, and experimental comparisons of direct dielectric methods and dye fluorescence methods could be useful for mixtures. For most accurate theoretical comparisons it is essential to characterize the ET parameters more fully than yet done for our system; often this requires studies of vibrational reorganization energy and solvent reorganization energy. A full quantum and molecular dynamics analysis could provide insight into the details of local solvation and contributions of the first solvation layer relaxation.

Acknowledgment. This work was supported by the U.S. Department of Energy, Office of Science (Grant DE-FG02-91ER14228).

References and Notes

(1) Bixon, M.; Jortner, J. Electron Transfer−From Isolated Molecules to Biomolecules. Part 1. In *Advances in Chemical Physics*; Jortner, J., Bixon, M., Eds.; John Wiley & Sons: New York, 1999; Vol. 106; p 35.

(2) Yoshihara, K. Electron Transfer−From Isolated Molecules to Biomolecules. Part 2. In *Advances in Chemical Physics*; Jortner, J., Bixon, M., Eds.; John Wiley & Sons: New York, 1999; Vol. 107; p 371.

(3) Newton, M. D. Electron Transfer−From Isolated Molecules to Biomolecules. Part 1. In *Advances in Chemical Physics*; Jortner, J., Bixon, M., Eds.; John Wiley & Sons: New York, 1999; Vol. 106; p 303.

(4) Garg, A.; Onuchic, J. N.; Ambegaokar, V. *J. Chem. Phys.* **1985**, *83*, 4491.

(5) Rips, I.; Jortner, J. *J. Chem. Phys.* **1987**, *87*, 6513.

(6) Zusman, L. D. *Chem. Phys.* **1980**, *49*, 295.

(7) Sumi, H.; Marcus, R. A. *J. Chem. Phys.* **1986**, *84*, 4894.

(8) Sparpaglione, M.; Mukamel, S. *J. Chem. Phys.* **1988**, *88*, 4300.

(9) Sparpaglione, M.; Mukamel, S. *J. Chem. Phys.* **1988**, *88*, 3263.

(10) Tominaga, K.; Walker, G. C.; Kang, T. J.; Barbara, P. F.; Fonseca, T. *J. Phys. Chem.* **1991**, *95*, 10485.

(11) McManis, G. E.; Weaver, M. J. *J. Chem. Phys.* **1989**, *90*, 912.

(12) Kang, T. J.; Kahlow, M. A.; Giser, D.; Swallen, S.; Nagarajan, V.; Jarzeba, W.; Barbara, P. F. *J. Phys. Chem.* **1988**, *92*, 6800.

(13) Horng, M. L.; Dahl, K.; Jones, G., II; Maroncelli, M. *Chem. Phys. Lett.* **1999**, *315*, 363.

(14) Heitele, H. *Angew. Chem., Int. Ed. Engl.* **1993**, *32*, 359.

(15) Kosower, E. M.; Huppert, D. *Annu. Rev. Phys. Chem.* **1986**, 127.

(16) Akesson, E.; Johnson, A. E.; Levinger, N. E.; Walker, G. C.; DeBruil, T. P.; Barbara, P. F. *J. Chem. Phys.* **1992**, *96*, 7859.

(17) Haberle, T.; Hirsch, J.; Pollinger, F.; Heitele, H.; Michel-Beyerle, M. E.; Staab, H. A. *J. Phys. Chem.* **1996**, *100*, 18269.

(18) Kobayashi, T.; Takagi, Y.; Kandori, H.; Kemnitz, K.; Yoshihara, K. *Chem. Phys. Lett.* **1991**, *180*, 416.

(19) Pal, H.; Nagasawa, Y.; Tominaga, K.; Yoshihara, K. *J. Phys. Chem.* **1996**, *100*, 11964.

(20) Sinks, L. E.; Wasielewski, M. R. *J. Phys. Chem. A* **2003**, *107*, 611.

(21) Moran, A. M.; Ponnu, A.; Spears, K. G. *J. Phys. Chem. A* **2005**, *109*, 1795.

(22) Jurczok, M.; Plaza, P.; Martin, M. M.; Meyer, Y. H.; Rettig, W. *Chem. Phys.* **2000**, *256*, 253.

(23) Kang, T. J.; Jarzeba, W.; Barbara, P. F. *Chem. Phys.* **1990**, *149*, 81.

(24) Kovalenko, S. A.; Pérez Lustres, J. L.; Ernsting, N. P.; Rettig, W. *J. Phys. Chem. A* **2003**, *107*, 10228.

(25) Akesson, E.; Walker, G. C.; Barbara, P. F. *J. Chem. Phys.* **1991**, *95*, 4188.

(26) Walker, G. C.; Akesson, E.; Johnson, A. E.; Levinger, N. E.; Barbara, P. F. *J. Phys. Chem.* **1992**, *96*, 3728.
(27) Kovalenko, S. A.; Eilers-König, N.; Senyushkina, T. A.; Ernsting, N. P. *J. Phys. Chem. A* **2001**, *105*, 4834.
(28) Hwang, H.; Rossky, P. J. *J. Phys. Chem. A* **2004**, *108*, 2607.
(29) Pugžlys, A.; den Hartog, H. P.; Baltuška, A.; Pshenichnikov, S.; Umapathy, S.; Wiersma, D. A. *J. Phys. Chem. A* **2001**, *105*, 11407.
(30) Tominaga, K.; Kliner, D. A. V.; Johnson, A. E.; Levinger, N. E.; Barbara, P. F. *J. Chem. Phys.* **1993**, *98*, 1228.
(31) Monk, P. M. S. *The Viologens: Physiochemical Properties, Synthesis and Applications of the Salts of 4,4′-Bipyridine*; John Wiley and Sons: New York, 1998.
(32) Marin, T. W.; Homoelle, B. J.; Spears, K. G.; Hupp, J. T.; Spreer, L. O. *J. Phys. Chem. A* **2002**, 1131.
(33) Reynolds, L.; Gardecki, J. A.; Frankland, S. J. V.; Horng, M. L.; Maroncelli, M. *J. Phys. Chem.* **1996**, *100*, 10337.
(34) Marcus, R. A.; Sutin, N. *Biochim. Biophys. Acta* **1985**, *811*, 265.
(35) Newton, M. D.; Sutin, N. *Annu. Rev. Phys. Chem.* **1984**, *35*, 437.
(36) Mühlbacher, L.; Egger, R. *J. Chem. Phys.* **2003**, *118*, 179.
(37) Mühlbacher, L.; Egger, R. *Chem. Phys.* **2004**, *296*, 193.
(38) Zhang, M. L.; Zhang, S.; Pollak, E. *J. Chem. Phys.* **2003**, *119*, 11864.
(39) Horng, M. L.; Gardecki, J. A.; Papazyan, A.; Maroncelli, M. *J. Phys. Chem.* **1995**, *99*, 17311.
(40) Kindt, J. T.; Schmuttenmaer, C. A. *J. Phys. Chem.* **1996**, *100*, 10373.
(41) Biswas, R.; Bagchi, B. *J. Phys. Chem. A* **1999**, *103*, 2495.
(42) Bingemann, D.; Ernsting, N. P. *J. Chem. Phys.* **1995**, *102*, 2691.
(43) Biswas, R.; Nandi, N.; Bagchi, B. *J. Phys. Chem. B* **1997**, *101*, 2968.
(44) Joo, T.; Jia, Y.; Yu, J.-Y.; Lang, M. J.; Fleming, G. R. *J. Chem. Phys.* **1996**, *104*, 6089.
(45) Venables, D. S.; Schmuttenmaer, C. A. *J. Chem. Phys.* **1998**, *108*, 4935.
(46) Venables, D. S.; Schmuttenmaer, C. A. *J. Chem. Phys.* **2000**, *113*, 11222.
(47) Venables, D. S.; Schmuttenmaer, C. A. *J. Chem. Phys.* **2000**, *113*, 3249.
(48) Eaton, G.; Pena-Nuñez; Symons, M. C. R. *J. Chem. Soc., Faraday Trans. 1* **1988**, *84*, 2181.
(49) Megehee, E. G.; Johnson, C. E.; Eisenberg, R. *Inorg. Chem.* **1989**, *28*, 2423.